Segmental Expression of the Bradykinin Type 2 Receptor in Rat Efferent Ducts and Epididymis and Its Role in the Regulation of Aquaporin 9[1]

C. Belleannée,[3] N. Da Silva,[3] W.W.C. Shum,[3] M. Marsolais,[4] R. Laprade,[4] D. Brown,[3] and S. Breton[2,3]

Center for Systems Biology,[3] Program in Membrane Biology/Nephrology Division, Massachusetts General Hospital, Boston, Massachusetts 02114
Groupe d'Étude des Protéines Membranaires,[4] Université de Montréal, Montréal, Québec, Canada H3C 3J7

ABSTRACT

Water and solute transport in the efferent ducts and epididymis are important for the establishment of the appropriate luminal environment for sperm maturation and storage. Aquaporin 9 (AQP9) is the main water channel in the epididymis, but its regulation is still poorly understood. Components of the kinin-kallikrein system (KKS), leading to the production of bradykinin (BK), are highly expressed in the lumen of the male reproductive tract. We report here that the epididymal luminal fluid contains a significant amount of BK (2 nM). RT-PCR performed on epididymal epithelial cells isolated by laser capture microdissection (LCM) showed abundant BK type 2 receptor (*Bdkrb2*) mRNA expression but no type 1 receptor (*Bdkrb1*). Double-immunofluorescence staining for BDKRB2 and the anion exchanger AE2 (a marker of efferent duct ciliated cells) or the V-ATPase E subunit, official symbol ATP6V1E1 (a marker of epididymal clear cells), showed that BDKRB2 is expressed in the apical pole of nonciliated cells (efferent ducts) and principal cells (epididymis). Triple labeling for BDKRB2, AQP9, and ATP6V1E1 showed that BDKRB2 and AQP9 colocalize in the apical stereocilia of principal cells in the cauda epididymidis. While uniform *Bdkrb2* mRNA expression was detected in the efferent ducts and along the epididymal tubule, marked variations were detected at the protein level. BDKRB2 was highest in the efferent ducts and cauda epididymidis, intermediate in the distal initial segment, moderate in the corpus, and undetectable in the proximal initial segment and the caput. Functional assays on tubules isolated from the distal initial segments showed that BK significantly increased AQP9-dependent glycerol apical membrane permeability. This effect was inhibited by BAPTA-AM, demonstrating the participation of calcium in this process. This study, therefore, identifies BK as an important regulator of AQP9.

bradykinin receptor, efferent ducts, epididymis, male reproductive tract, water channel

INTRODUCTION

Bradykinin (BK) is one of the most important peptides regulating water and ionic balance in the body [1, 2]. BK and the more stable kinin, kallidin (Lys-BK), are part of the kinin-kallikrein system (KKS). They are generated from the partial proteolysis of kininogen precursors by plasma or tissue kallikreins [3]. Most of the physiological activities induced by kinins are mediated by two receptors belonging to the G-protein-coupled receptor family: the BK receptor B1 (BDKRB1), whose expression is induced by inflammation, and the BK receptor B2 (BDKRB2). BDKRB2 mediates the action of BK and Lys-BK, and BDKRB1 mediates the action of their respective metabolites desArg^{9}BK and desArg^{10}-kallidin (for review see [4] and [5]). Activation of both receptors induces the release of intracellular calcium from internal stores via phospholipase C (PLC) activation (reviewed in [5]).

In the male reproductive tract, most of the components of the KKS are present and regulate important functions related to reproduction and fertility. BK has been reported to act on pre-spermatogonial cell proliferation in vitro [6], on anion secretion in the epididymis and vas deferens [7, 8], on smooth-muscle contraction and prostaglandin production in the vas deferens [9], and on the motility and vitality of ejaculated spermatozoa [10–12]. The activation of anion secretion by BK was shown to be mediated by BDKRB2 in epididymal cells and vas deferens cells in culture [7, 8]. Interestingly, Lys-BK triggers two different pathways depending on the side of the cell where this kallidin is applied: on the basolateral side, the kallidin effect is COX-dependent, whereas on the apical side it is Ca^{2+} dependent [7, 13].

In the efferent ducts and epididymis, water and solute transport are essential for establishing the proper luminal environment for sperm maturation and storage. Significant water reabsorption occurs in these organs and participates in the concentration of spermatozoa and the establishment of luminal hypertonicity [14–20]. In the distal regions of the epididymis and in the vas deferens, anion-driven water secretion occurs and helps to control the final fluidity of the luminal content [21, 22]. In addition, glycerol—a sperm metabolic substrate—is accumulated in the lumen of the epididymis [23]. Both water and glycerol transport occur via the aquaglyceroporin AQP9 [24–26], which is highly expressed in the apical membrane of epididymal principal cells and efferent duct nonciliated cells [27–30].

Previous studies have shown the expression of *Bdkrb2* mRNA and protein in rat testis and prostate [31, 32]. However, while the *Bdkrb2* gene was shown to be expressed in the epididymis [32], there is no evidence to date on the presence of this receptor at the protein level in this organ. In the present study, we characterized *Bdkrb2* mRNA expression in epithelial cells of rat epididymis, and we localized BDKRB2 protein in efferent ducts and epididymis by Western blotting and

immunofluorescence. In addition, the functional role of BDKRB2 on glycerol transport in response to luminal BK was investigated in epididymal tubules isolated and perfused in vitro.

MATERIALS AND METHODS

Enzyme-Linked Immunosorbent Assay

BK was measured in rat epididymal luminal fluid using a competitive enzyme immunoassay system (Bradykinin EIA Kit; Phoenix Pharmaceuticals, Inc., Burlingame, CA). Epididymal luminal fluid and spermatozoa were collected by luminal microperfusion of the cauda epididymidis, a procedure that is routinely performed in our laboratory [33–35] and ensures minimal cell and blood contamination.

Sprague-Dawley rats (Charles River Laboratories, Wilmington, MA) were acquired, retained, and used in compliance with the Institutional Animal Care and Use Committees of the Massachusetts General Hospital and the University of Montreal. Sexually mature male rats were anesthetized with Nembutal (65 mg/kg body weight, i.p.; Ovation Pharmaceuticals Inc.), and the epididymis and vas deferens were exposed. A small incision was made in the proximal cauda epididymidis to insert a small microcannula (approximately 0.4-mm outer diameter, 0.2-mm inner diameter) into the lumen. The vas deferens was cut and a small tubule was adapted and fixed in place to collect the luminal content. The cauda epididymidis and the proximal vas deferens were perfused with PBS (0.9% NaCl in 10 mM sodium phosphate buffer, pH 7.4) at a rate of 45 μl/ml using a syringe pump (Model 100; KD Scientific, Inc., Holliston, MA). Epididymal fluids were collected from three rats and separated from spermatozoa by two consecutive centrifugations at $10\,000 \times g$ each. Supernatants were then stored at $-20°C$ until further use.

The detection of BK in epididymal fluid was performed separately for each animal according to the procedure provided by the ELISA kit manufacturer. Each sample was analyzed in triplicate, and absorbance optical density values were read at 450 nm on a Microtiter Plate Reader (DTX 880, Multimode Detector; Beckman Coulter). BK concentration was assessed by extrapolation of the standard curve made from dilutions of known BK concentration.

Antibodies

To localize the vacuolar H^+ATPase (also known as V-ATPase) along the male reproductive tract, an affinity-purified polyclonal antibody against the last 10 amino acids (CGANANRKFLD) of the C-terminal domain of ATP6V1E1 was used [36–38]. An affinity-purified, polyclonal antibody against the C-terminal domain of human BDKRB2 was purchased from Sigma (Catalog #B-5685; St. Louis, MO). A blocking peptide corresponding to the C-terminal region of BDKRB2 was purchased from Santa Cruz (Catalog #sc-15050P; Santa Cruz, CA) and used for competition studies with the anti-BDKRB2 antibody. An affinity-purified rabbit polyclonal antibody raised against a peptide corresponding to the last 15 amino acids (PSENNLEKHELSVIM) of the C-terminal tail of rat AQP9 was used. This antibody has been previously characterized [30, 39]. To identify the ciliated cells in the efferent ducts, an affinity-purified rabbit antibody raised against the Cl/HCO_3 AE2 exchanger (provided by Seth Alper, Beth Israel Deaconess Medical Center, Boston, MA) was used [40, 41].

The following affinity-purified secondary antibodies were purchased from the Jackson ImmunoResearch Laboratories (West Grove, PA) and were used as appropriate: 1) goat anti-rabbit (IgG, H&L) conjugated to fluorescein isothiocyanate (GAR-FITC); 2) a donkey anti-rabbit (IgG, H&L) conjugated to indocarbocyanine 3 (DAR-Cy3); 3) a donkey anti-chicken (IgG, H&L) conjugated to FITC (DAC-FITC); and a donkey anti-chicken (IgG, H&L) conjugated to indocarbocyanine 5 (DAC-Cy5).

Tissue Fixation and Immunofluorescence

Sexually mature male rats were anesthetized with Nembutal (65 mg/kg body weight, i.p.) and perfused via the left ventricle with PBS followed by fixative containing 4% paraformaldehyde, 10 mM sodium periodate, 75 mM lysine, and 5% sucrose in 0.1 M sodium phosphate buffer (PLP), as described previously [30, 38]. The reproductive tract was removed and kept in the same fixative overnight at 4°C, followed by extensive rinsing in PBS. The tissues were kept in PBS (containing 0.02% NaN_3) at 4°C until further use.

To cut frozen sections, tissues were infiltrated with 30% sucrose in PBS for several hours, mounted for cryosectioning in Tissue-Tek OCT compound 4583 (Sakura Finetek USA, Inc., Torrance, CA), and quick-frozen. Sections were cut at 5 μm using a Leica 3050 cryotome (Spencer Scientific, Derry, NH) and picked up onto Superfrost/Plus microscope slides (Fisher Scientific, Pittsburgh, PA).

For indirect immunofluorescence microscopy, sections were hydrated for 15 min in PBS and treated for 4 min with 1% SDS [42]. Sections were washed in PBS for 5 min and then blocked in PBS containing 1% BSA for 15 min. Primary antibody against BDKRB2 (3.3 μg/ml, diluted in DAKO diluent; DAKO Corp., Carpinteria, CA) was applied in a moist chamber for 90 min at room temperature or overnight at 4°C. Sections were washed in high-salt PBS (2.7% NaCl) twice for 5 min and once in normal PBS. Secondary antibody DAR-CY3 (1.9 μg/ml in DAKO) was then applied for 1 h at room temperature followed by washes, as described above. Some epididymis sections were double-stained by subsequent incubation with our affinity-purified antibody against ATP6V1E1 (5.5 μg/ml in DAKO), followed by DAC-FITC (25 μg/ml in DAKO). Slides were mounted in Vectashield medium containing 4′,6′-diamidino-2-phenylindole (DAPI; Vector Laboratories, Inc., Burlingame, CA). The specificity of the anti-BDKRB2 antibody was tested by incubating sections with the primary antibody that had been preincubated in the presence of a 10-fold (wt/wt) excess of the BDKRB2 peptide for 1 h at room temperature prior to application.

Some sections were triple-stained for BDKRB2, AQP9, and ATP6V1E1. Because the anti-BDKRB2 and anti-AQP9 antibodies were both raised in rabbit, an amplification procedure that allows staining of sections with two primary antibodies raised in the same species was used, as we have previously described [43]. Briefly, anti-BDKRB2 was first applied at a concentration that is too low to be detected by conventional staining (0.5 μg/ml). This diluted antibody was detected using a tyramide signal amplification kit (PerkinElmer Life and Analytical Sciences, Boston, MA) with tyramide-CY3 as a fluorescent reagent, according to the manufacturer's instructions. The sections were then incubated conventionally with anti-AQP9 (2.8 μg/ml in DAKO) and secondary GAR-FITC (25 μg/ml in DAKO), followed by anti-ATP6V1E1 and DAC-Cy5 (75 μg/ml in DAKO).

Some efferent duct sections were double-stained to identify the ciliated and nonciliated cells in this epithelium. Sections were first incubated overnight with the BDKRB2 antibody, followed by washes and incubation with the appropriate secondary antibody, as described in detail above. Anti-AE2 antibody (0.8 μg/ml in DAKO) was then applied at room temperature for 2 h. After rinsing in PBS, sections were incubated with GAR-FITC for 1 h and mounted in Vectashield.

Digital images were acquired using a Nikon Eclipse 800 epifluorescence microscope (Nikon Instruments, Inc., Melville, NY) with a Hamamatsu Orca 100 CCD camera (Hamamatsu, Bridgewater, NJ), analyzed using IPLab scientific image processing software (Scanalytics, Inc., Fairfax, VA), and imported into Adobe Photoshop image editing software (Adobe Systems, Inc., San Jose, CA). Some images were acquired using a Zeiss Radiance 2000 confocal microscope (Carl Zeiss Microimaging Inc.) using LaserSharp 2000 version 4.1 software (BioRad) and were imported into Adobe Photoshop software as TIFF files.

SDS-PAGE and Western Blotting

Total protein extracts from whole epididymides were denatured and reduced by boiling in NuPAGE LDS Sample Buffer in the presence of NuPAGE Reducing Agent (Invitrogen, Carlsbad, CA) for 5 min. Proteins (50 μg per lane) were loaded onto SDS-PAGE Tris-glycine polyacrylamide 8%–16% gradient gels (Novex precast gels; Invitrogen) and transferred onto Immun-Blot polyvinylidene difluoride membranes (Bio-Rad Laboratories, Hercules, CA) using the Bio-Rad system. Membranes were blocked in Tris-buffered saline (TBS) containing 5% nonfat dry milk and then incubated overnight at 4°C with anti-BDKRB2 antibody (0.2 μg/ml) diluted in TBS containing 2.5% milk. After three washes in TBS with 0.1% Tween 20 and a 15-min block in TBS with milk, membranes were incubated with a donkey anti-rabbit IgG conjugated to horseradish peroxidase (Jackson ImmunoResearch Laboratories) for 1 h at room temperature. After three further washes, antibody binding was detected with the Western Lightning Chemiluminescence reagent (PerkinElmer) and Kodak X-Omat blue XB-1 films (Henry Schein Inc.). Peptide inhibition controls were performed using the same protocol after preincubation of the anti-BDKRB2 antibody in the presence of a 10-fold (wt/wt) excess of the BDKRB2 peptide for 1 h at room temperature prior to incubation with the membrane.

Laser Capture Microdissection

Laser capture microdissection (LCM) was performed on adult rat epididymal epithelium. These samples were used and characterized in our previous study [44] and contain a total population of epithelial cells with minimum contamination from surrounding smooth-muscle cells, interstitial tissues, blood vessels, and spermatozoa. Briefly, epididymides were dissected, frozen on dry ice, and sectioned at 6 μm. Sections were picked up onto uncoated glass slides and were stained for 30 sec in Mayer hematoxylin,

LCM

Bdkrb2   Bdkrb1   NTC

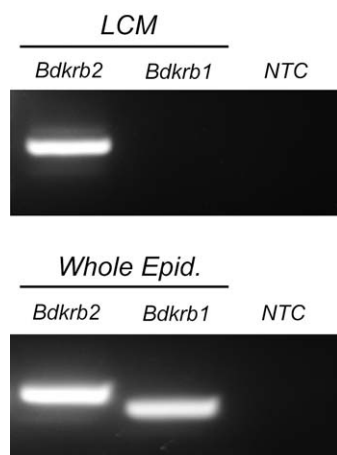## Whole Epid.

Bdkrb2   Bdkrb1   NTC

FIG. 1. RT-PCR analysis of *Bdkrb1* and *Bdkrb2* expression in epithelial cells of adult rat epididymis. Top panel: Epithelial cells were isolated by LCM and used as templates for conventional RT-PCR analysis. A strong signal was obtained for the *Bdkrb2* transcript, but no *Bdkrb1* was detected. Bottom panel: Strong *Bdkrb2 and Bdkrb1* signals were obtained in a whole epididymis mRNA extract. NTC, No template control.

followed by dehydration in 70%, 95%, and 100% ethanol. Slides were dipped in xylene twice for 5 min and air-dried. Epithelial cells were harvested by using the PixCell II LCM system (Arcturus Engineering, Mountain View, CA) with the following parameters: spot size 7.5 μm, pulse duration 1.5 msec, power 40–60 mW. Each LCM sample used 2000–4000 laser pulses, which corresponded to approximately 2000–4000 epithelial cells.

Total RNA Extraction, RNA Amplification, and Reverse Transcription

LCM samples were treated as we have previously described [44]. Briefly, total RNA was extracted following the PicoPure RNA Isolation kit protocol (Molecular Devices). DNase treatment was performed in a purification column using the RNase-Free DNase set (Qiagen, Valencia, CA). The RNA samples were amplified by a T7-based process derived from the Eberwine method using the RiboAmp RNA Amplification kit (Molecular Devices). The quality of aRNA was assessed by gel electrophoresis. After two rounds of amplification, the bulk of the aRNA product was 200–600 bp in length. On average, 70 μg of aRNA was generated from each LCM sample.

Total RNA was also isolated from distinct regions (efferent ducts, initial segment, caput, corpus, and cauda) and from whole epididymides. Tissues were frozen in liquid nitrogen immediately after dissection and homogenized in RNAwiz (Ambion, Austin, TX), and RNA was extracted following the manufacturer's protocol. Genomic DNA contamination was removed using the DNA-free kit (Ambion). The integrity of total RNA samples was assessed by separating 0.5 μg of each extract on an RNA 6000 Nano Total RNA chip with the Agilent 2100 bioanalyzer (Agilent Technologies, Inc.) following the manufacturer's protocol. DNA-free aRNA and total RNA samples were aliquoted and stored at −80°C.

Amplified aRNA (3 μg) was converted into first-strand cDNA for 1 h at 37°C with 1× first-strand buffer adjusted to pH 8.3 and containing 50 mM Tris-HCl, 75 mM KCl, 3 mM MgCl$_2$, 10 mM dithiothreitol, 6 ng/μl random hexamers, 500 μM each dNTP, 50 U RNase inhibitor (Promega, Madison, WI), and 400 U SuperScript II reverse transcriptase (Invitrogen), as we have described previously [44]. Second-strand synthesis was performed for 2 h at 16°C with 1× second-strand buffer adjusted to pH 6.9 and containing 20 mM Tris-HCl (pH 6.9), 90 mM KCl, 4.6 mM MgCl$_2$, 0.15 mM β-NAD$^+$, 10 mM (NH$_4$)$_2$SO$_4$, 250 μM each dNTP, 40 U DNA polymerase I, 2 U *Escherichia coli* RNase H, and 10 U *E. coli* DNA ligase (all reagents from Invitrogen). Double-stranded DNA was purified with the Qiaquick PCR purification kit (Qiagen) and quantified with the PicoGreen dsDNA quantification reagent (Molecular Probes, Eugene, OR) by using a spectrofluorometer.

End-Point and Quantitative PCR

Conventional end-point PCR was performed as we have described previously [44]. Two nanograms of reverse-transcription templates were mixed with 1.25 U AmpliTaq Gold DNA polymerase (Applied Biosystems, Foster

City, CA), 50 mM KCl, 10 mM Tris-HCl (pH 8.3), 2.0 mM MgCl 2, 1.0 mM each dNTP, and 0.5 μM forward and reverse oligonucleotide primers. PCR was performed in a Flexigene thermal cycler (Techne, Princeton, NJ) with the following parameters: 8 min at 95°C to activate the polymerase, followed by 30–40 cycles of melting for 1 min at 95°C, annealing for 30 sec at 60°C, extension for 45 sec at 72°C, and a final extension for 10 min at 72°C. PCR products were resolved in a 2.5% agarose gel containing GelStar stain (Lonza, Rockland, ME). A no-template control (NTC) was included in each PCR plate. Oligonucleotide primer pairs were designed using the OligoPerfect Designer software (Invitrogen) to amplify a short sequence in the 3′ end of the rat BK receptor cDNAs. Primers were synthesized by Invitrogen. Sequences of primers used for the PCR were 5′-AAA TGA TGC AAC CGA GAA GC-3′ (forward) and 5′-TCA GCT GAC CAG ATG GTC TTT-3′ (reverse) for *Bdkrb1*, 5′-CAC TGC AGG GTC TGC AAC TA-3′ (forward) and 5′-CAG AGT GCT CCT CCC TTG TC-3′ (reverse) for *Bdkrb2*, and 5′-AGA GAG AGG CCC TCA GTT GCT-3′ (forward) and 5′-TGG AAT TGT GAG GGA GAT GCT-3′ (reverse) for *Gapdh*.

Quantitative PCR analysis of *Bdkrb2* expression in the different epididymal regions was performed as we have described previously [44] with an ABI PRISM 7900HT Sequence Detection System (Applied Biosystems). Each reaction was performed in triplicate by using 5 ng of cDNA from each sample and the iTaq SYBR Green Supermix with ROX reagent (Bio-Rad). Quantitative PCR analysis was performed for *Gapdh* in the same extracts. Expression of *Bdkrb2* was normalized to *Gapdh* values. Data were calculated from three experiments. A dissociation curve was generated after each SYBR Green PCR run to further confirm the specificity of the amplification. Primers were the same as the ones used for conventional end-point PCR described above.

Functional Studies on Epididymal Tubules Perfused In Vitro

Epididymal tubules were dissected from the distal initial segment, a region where the surrounding muscle cell layer is thinner compared to tubules of the more distal regions, and where detectable levels of BDKRB2 were observed. A lower peristaltic activity in tubules from the initial segment greatly facilitates their microscope visualization compared to tubules of the cauda epididymidis. Peritubular and luminal perfusions were performed on tubules transferred into a perfusion chamber mounted on the stage of an Olympus IMT-2 inverted microscope, as we have previously described [25, 40]. After an initial control period, the apical membrane permeability to glycerol was estimated from the initial rate of increase in cellular volume induced following the isotonic replacement of 60 mM raffinose (an impermeant solute in epididymal epithelial cells) with 60 mM glycerol. Digital pictures were captured at 15-sec or 30-sec intervals using a Nikon Coolpix 995 camera and were analyzed using IPLab software (Scanalytics, Fairfax, VA). The height of epithelial cells was measured for each time point at five different locations along the tubule, and the values were averaged as we have described previously [25]. These values were used to assess cell volume expressed as percentage of initial control volume. Initial rates of cell swelling were determined from four cell volume values measured during the first minute of glycerol exposure at 15-sec intervals. The effects of 1 μM BK alone or in the presence of BAPTA-AM (5 μM) or phloretin (500 μM) were examined on glycerol-induced cell swelling. Statistical analysis was performed using the Student *t*-test for paired experiments.

RESULTS

BK Detection in Rat Epididymal Fluid

The presence and concentration of BK were assessed by competitive enzyme immunoassay performed on the epididymal luminal fluid of three adult rats. On average, 2.27 ± 0.74 ng/ml (mean ± SEM) of BK was detected, corresponding to a concentration of 2.14 ± 0.69 nM.

Expression of Bdkrb2 mRNA in Epithelial Cells of Adult Rat Epididymis

Expression of the mRNA encoding the BK receptors *Bdkrb1* and *Bdkrb2* was investigated by RT-PCR using mRNA extracts from epithelial cells isolated by LCM from adult rat epididymides (Fig. 1, top panel) and from whole epididymides (Fig. 1, bottom panel). In agreement with previous studies [32], *Bdkrb2* mRNA was readily detectable in epithelial cells of the epididymis. In marked contrast, *Bdkrb1* mRNA was not found
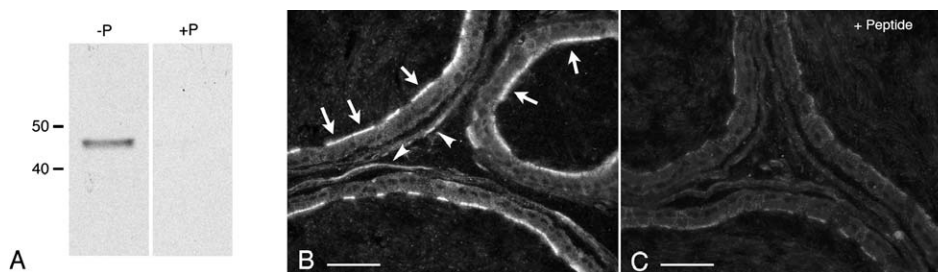
FIG. 2. Detection of BDKRB2 in rat epididymis. **A**) Western blot with anti-BDKRB2 antibody in whole epididymis protein extract (50 μg per lane). A single band at about 45 kDa was detected using the native antibody (-P) and was abolished when the antibody was preabsorbed with the immunizing peptide (+P). **B**, **C**) Immunofluorescence staining for BDKRB2 on rat cauda epididymidis sections. Intense labeling was detected in the apical pole of many epithelial cells (**B**, arrows). Smooth-muscle cell labeling was also visible (arrowheads). The staining was abolished after preincubation of the antibody with the BDKRB2 peptide (**C**). Images were acquired at the same exposure time. Bars = 20 μm.

in the same epithelial cell preparation. Both *Bdkrb1* and *Bdkrb2* were detected in whole epididymis extracts.

Detection of BDKRB2 by Western Blotting

By Western blotting, the anti-BDKRB2 antibody detected a single band at about 45 kDa corresponding to the expected molecular mass of BDKRB2 (Fig. 2A, left lane). Specificity of the antibody for BDKRB2 was confirmed by preincubation of the primary antibody with the BDKRB2 peptide prior to performing the Western blot on the same epididymal extracts. The 45-kDa band intensity was completely abolished (Fig. 2A, right lane), showing specificity of the antibody for BDKRB2. Native BDKRB2 was shown to be glycosylated in some tissues [45, 46]. In our study, the presence of a single, sharp, 45-kDa band indicates that this receptor does not appear to be significantly glycosylated in the epididymis.

Immunofluorescence Localization of BDKRB2

Immunofluorescence labeling showed abundant expression of BDKRB2 in the apical pole of many epithelial cells of the rat cauda epididymidis (Fig. 2B; arrows). No staining was detected in the basolateral membrane of epithelial cells, but, in agreement with data previously published [47], a faint labeling was seen in the surrounding smooth-muscle cell layer (arrowheads). The BDKRB2 staining was abolished when sections were incubated with antibody that had been preabsorbed with the peptide (Fig. 2C), confirming specificity of the anti-BDKRB2 antibody.

The discontinuous apical BDKRB2 staining of the epididymal epithelium suggested that its expression was restricted to one cell population. To identify the cell type positive for BDKRB2, double labeling for ATP6V1E1, a marker of clear cells [36–38], was performed (Fig. 3). A strong apical BDKRB2 labeling (red) was detected in ATP6V1E1-negative cells (arrows), identifying these cells as principal cells. ATP6V1E1-positive clear cells (green) did not show any detectable BDKRB2 labeling. Here again, BDKRB2 staining was detected in smooth-muscle cells surrounding the cauda epididymal tubule (arrowheads).

Segmental Expression of BDKRB2 in the Efferent Ducts and Along the Epididymal Tubule

By immunofluorescence, the levels of BDKRB2 expression showed significant variations along the epididymal tubule and in the efferent ducts. To compare expression in the different parts of the epididymis and the efferent ducts, sections of these regions were incubated at the same time using the same

procedure, and digital images were acquired with identical exposure time. BDKRB2 shows the highest levels of expression in the apical pole of epithelial cells in the efferent ducts (Fig. 4, A and B) and in the cauda region of the epididymis (Fig. 4F). A very well-defined boundary exists between the efferent ducts, where BDKRB2 is strongly expressed, and the proximal initial segment, where it is not detectable (Fig. 4B). In the distal initial segment, BDKRB2 is expressed at a moderate level (Fig. 4C), but it is not detectable in the caput epididymidis (Fig. 4D). BDKRB2 expression progressively increases from the mid corpus (Fig. 4E) to the cauda epididymidis (Fig. 4F).

Bdkrb2 mRNA expression was assessed in the efferent ducts and in four epididymal regions by conventional and quantitative RT-PCR (Fig. 5, A and B). Epididymides were subdivided into distal efferent ducts, initial segment, caput, corpus, and cauda. End-point PCR for *Bdkrb2* normalized for *Gapdh* showed no significant variation of expression in the efferent ducts and epididymis regions (Fig. 5A). This was confirmed by quantitative PCR analysis (Fig. 5B). Altogether these data indicate that the significant variations of BDKRB2 expression observed by immunofluorescence (Fig. 4, A–F) do not correlate with *Bdkrb2* mRNA expression.

Localization of BDKRB2 in Nonciliated Cells of the Efferent Ducts

Confocal microscopy imaging showed similar BDKRB2 immunostaining intensity in the proximal (p-ED) and distal (d-ED) efferent ducts (Fig. 6, A and B). While most epithelial cells were stained in their apical pole for BDKRB2, a subpopulation of cells appeared negative (arrows). To identify the cell type positive for BDKRB2, double immunostaining was performed for the anion exchanger AE2, which we have previously described as a marker of ciliated cells [40, 41]. High-magnification confocal imaging showed intense BDKRB2 labeling (red) in the apical membrane of nonciliated cells (negative for AE2) of the distal efferent ducts (Fig. 6C, red), whereas no BDKRB2 was detected in ciliated cells (arrow), which express AE2 (green) in their basolateral membrane. The same pattern of expression was observed in the proximal efferent ducts (data not shown). These results indicate expression of BDKRB2 in the apical membrane of nonciliated cells of the efferent ducts.

Colocalization of BDKRB2 and AQP9 in the Apical Membrane of Principal Cells of the Cauda Epididymidis

To determine the subcellular localization of BDKRB2, triple staining of cauda epididymidis sections for BDKRB2 (Fig. 7C;
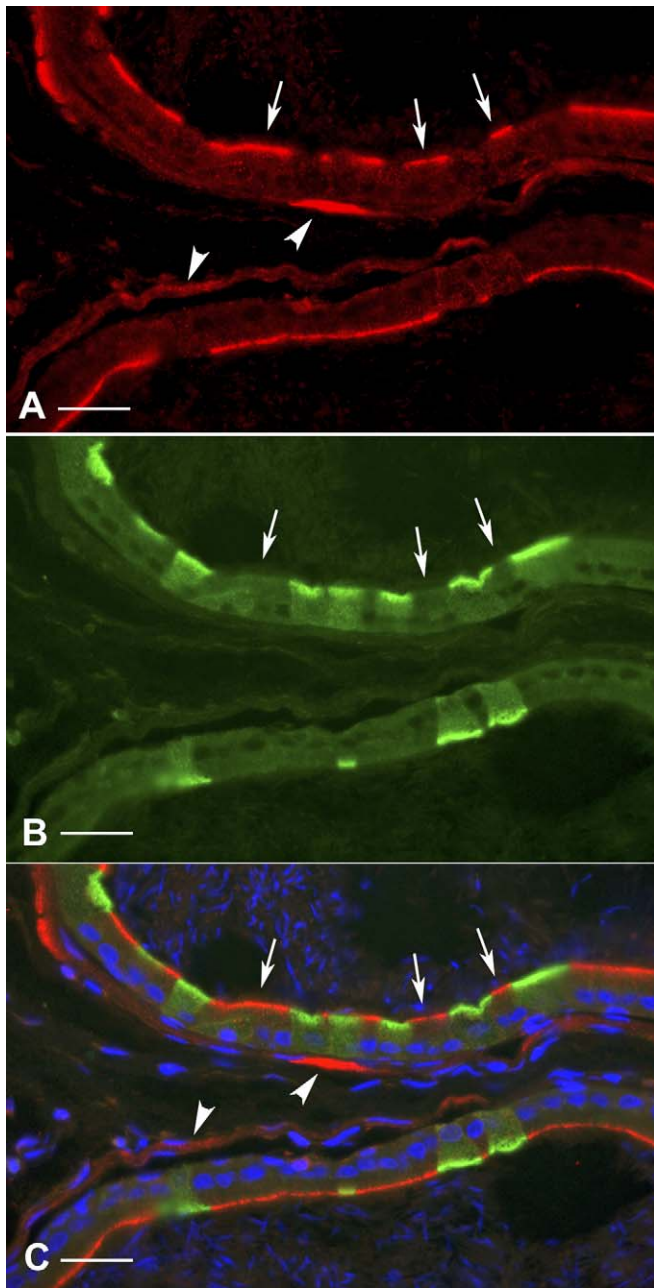
FIG. 3. Cellular localization of BDKRB2 in the cauda region of rat epididymis. Double labeling for ATP6V1E1 (**A**, red) and BDKRB2 (**B**, green) revealed that principal cells (negative for ATP6V1E1; arrows) express BDKRB2 in their apical pole, and that clear cells (positive for ATP6V1E1) are negative for BDKRB2. **C**) Merged panel. Smooth-muscle cells are also labeled (arrowheads). Nuclei are labeled blue with DAPI. Bars = 20 μm.

red), AQP9 (Fig. 7B; green), and ATP6V1E1 (Fig. 7D; blue) was performed. The merged panel shown in Figure 7A revealed that BDKRB2 colocalizes with AQP9 in the apical membrane of principal cells (yellow) and confirms that BDKRB2 is absent from clear cells, which are positive for ATP6V1E1.

Functional Role of BDKRB2 in the Epididymis

Activation of AQP9-dependent glycerol transport. We have previously shown a significant AQP9-dependent apical glycerol permeability in epididymal principal cells [26]. We tested here whether BK, a specific agonist for BDKRB2, might be involved in the regulation of this pathway. Epididymal tubules isolated from distal initial segments were luminally perfused with a control solution containing raffinose, a solute to which epididymis epithelial cells are impermeant. After a 5-min control period, isotonic replacement of 60 mM raffinose by 60 mM glycerol, which permeates through AQP9, was performed as we have described previously [25] (Fig. 8). Apical membrane glycerol permeability was estimated from the initial rate of cell swelling induced by this maneuver. Cell volume was estimated from the averaged height of epithelial cells measured at five different locations along the tubule. In agreement with our previous study [25], significant cell swelling was observed upon glycerol addition, indicating high permeability of the epididymal apical membrane to this neutral solute (Fig. 8A, Gly). On average, the initial rate of cell swelling was 17.8% ± 2.9% per minute (n = 7; Fig. 8B, left bars, GLY). After a postcontrol period in the absence of glycerol, BK (1 μM) was added into the luminal perfusate for a period of 5 min (Fig. 8A, BK), followed by a subsequent 5-min pulse of 60 mM glycerol still in the presence of BK (Fig. 8A, BK + Gly). While BK alone did not induce any change in cell volume, it significantly increased the initial rate of glycerol-induced cell swelling to 46.2% ± 10.8% per minute ($P < 0.001$; Fig. 8B, GLY + BK). We have previously shown that two consecutive glycerol pulses induced identical rates of cell swelling [25]. Thus, our data show that BK induced a 2.6-fold increase in glycerol-induced cell swelling compared to control (inset in Fig. 8A).

Role of calcium in the BK-induced increase in glycerol permeability. A previous study has shown that when applied to the apical side of cultured epididymal cells, BK triggers the release of calcium from intracellular stores [7]. To test for the role of calcium in the BK-induced increase in glycerol permeation, the effect of BK was examined in the presence of the calcium chelator BAPTA-AM. Epididymal tubules were submitted to two consecutive 60-mM glycerol pulses as described above. Five minutes prior to performing the second glycerol pulse, BK (1μM) was added into the luminal perfusate together with BAPTA-AM (5 μM). The second glycerol pulse was then applied still in the presence of BK and BAPTA-AM. As shown in Figure 8B (middle bars), BAPTA-AM counteracted the effect of BK on glycerol permeability (21.4% ± 2.4% per minute vs. 18.2% ± 5.4 % per minute, GLY vs. GLY + BK + BAPTA-AM, respectively; $P = 0.54$).

Participation of AQP9 in the BK-activated glycerol permeability. In order to confirm the participation of AQP9 in the BK-activated glycerol permeability, the effect of BK was examined in the presence of the AQP9 inhibitor phloretin [25]. Epididymal tubules were subjected to two consecutive 60-mM glycerol pulses as described above. Five minutes prior to performing the second glycerol pulse, BK (1μM) was added into the luminal perfusate together with phloretin (500 μM). The second glycerol pulse was then applied, still in the presence of BK and phloretin. As shown in Figure 8B (right bars), glycerol uptake was almost completely abolished in the presence of both BK and phloretin (2.47% ± 1.47% per minute vs. 20.52% ± 2.87% per minute, GLY + BK + phloretin vs. GLY, respectively; $P = 0.00029$).

Altogether, these data show that BK significantly increased the glycerol permeability of epithelial cells in a calcium-dependant manner via activation of AQP9.

DISCUSSION

While the main components of the KKS have been described in the epididymis, their role in modulating
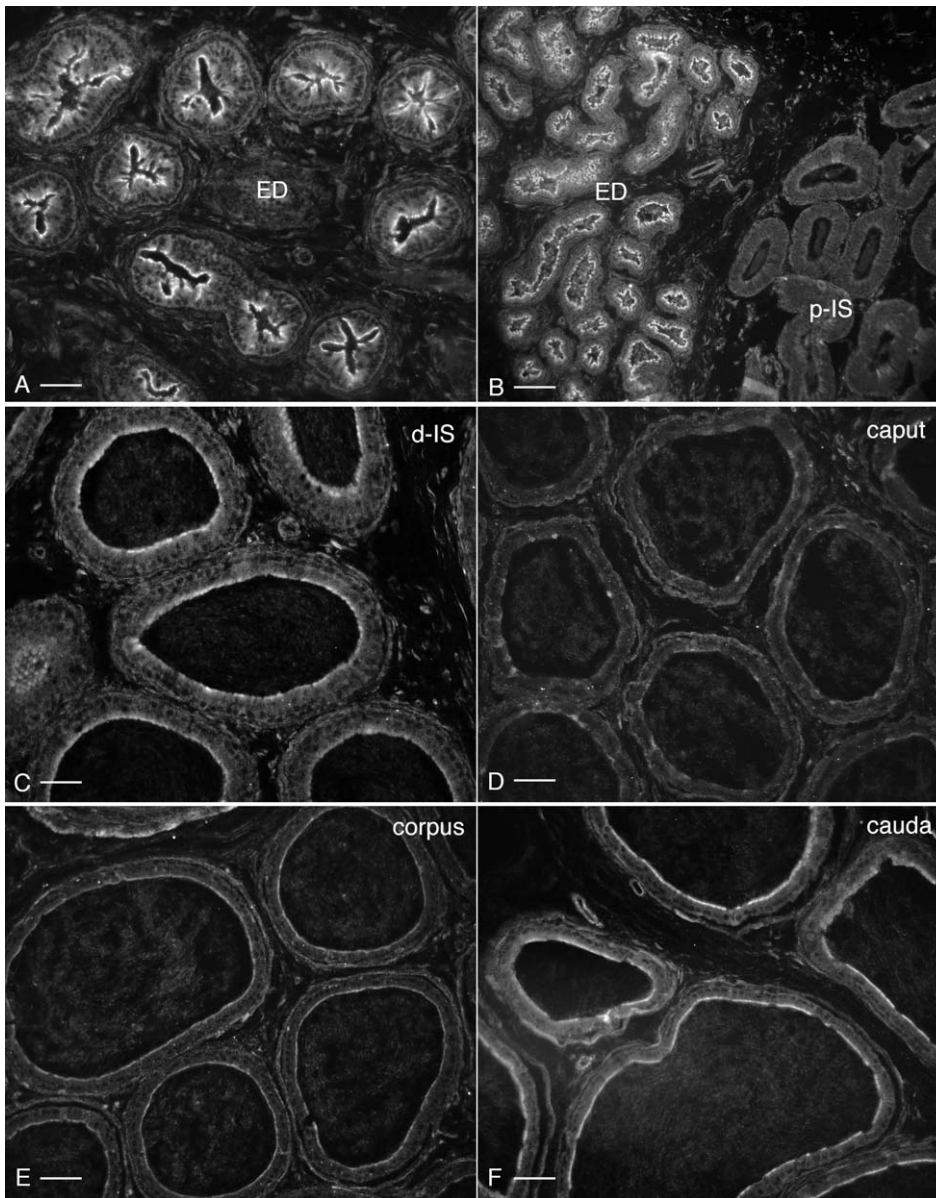
FIG. 4. Localization of BDKRB2 in efferent ducts and throughout the epididymis. Digital images were acquired with identical parameters to allow comparison of the levels of BDKRB2 expression among different regions. **A**) Distal efferent ducts (ED). **B**) Transition zone between distal efferent ducts and proximal initial segment (p-IS). **C**) Distal initial segment (d-IS). **D**) Caput. **E**) Corpus. **F**) Cauda. Stronger staining patterns are seen in the efferent ducts and cauda epididymidis. Intermediate staining is detected in the distal initial segments. Moderate staining is seen in the corpus epididymidis, and no significant labeling is detected in the proximal initial segment and caput epididymidis. Bars = 30 μm (**A**), 60 μm (**B**), 20 μm (**C**), and 25 μm (**D–F**).

transepithelial water and solute transport in this organ still remains elusive. The present study shows that the luminal fluid of the epididymis contains a significant concentration of BK and that the BK receptor, BDKRB2, is highly expressed in the apical membrane of nonciliated cells of the efferent ducts and of principal cells in some regions of the epididymis. Our results also show that luminal BK increases apical membrane glycerol permeability in the distal initial segment of the epididymis, an effect that is mediated by intracellular calcium and occurs via the activation of the aquaglyceroporin AQP9.

Most of the physiological activities of BK are mediated by BDKRB2, which exhibits a higher affinity for this peptide than
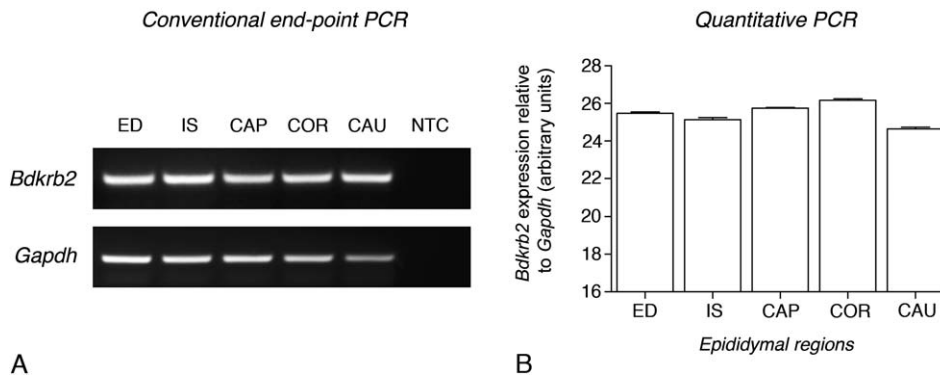

FIG. 5. RT-PCR analysis of *Bdkrb2* expression in the efferent ducts (ED) and in different epididymal regions: initial segment (IS), caput (CAP), corpus (COR) and cauda (CAU). Analysis was performed both by conventional end-point (**A**) and quantitative (**B**) PCR. *Bdkrb2* expression normalized for *Gapdh* was relatively constant in the ED and the different epididymal regions. *Gapdh*, Loading controls using primer sets specific for GAPDH; NTC, no template control.
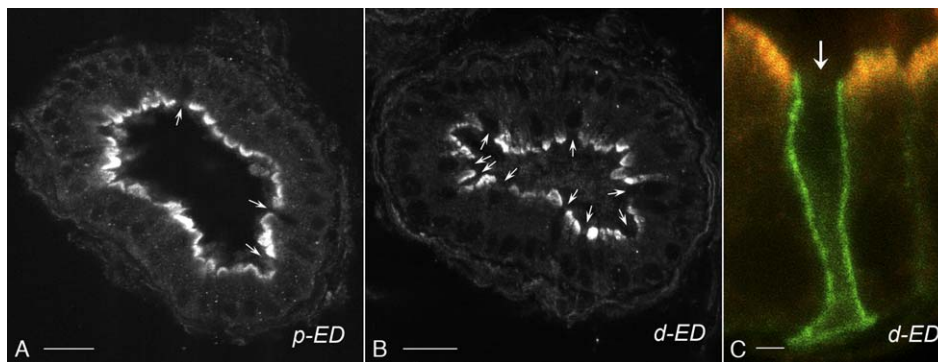
FIG. 6.   Confocal image of cellular localization of BDKRB2 in the efferent ducts. Immunostaining for BDKRB2 was performed in the proximal (**A**; *p-ED*) and distal efferent ducts (**B**; *d-ED*). Pictures were acquired using the same parameters. Similar staining intensity was detected in both segments. BDKRB2 is localized in the apical membrane of most epithelial cells. Some cells are negative for BDKRB2 (arrows). **C**) Double labeling for BDKRB2 (red) and the ciliated cell marker AE2 (green) was performed in the d-ED. Intense BDKRB2 labeling was detected in the apical membrane of nonciliated cells. No staining was detected in ciliated cells identified by their basolateral staining for AE2 (arrow). Bars = 30 μm (**A**, **B**) and 3 μm (**C**).

BDKRB1, whose expression is induced by pro-inflammatory factors [5]. In the male reproductive tract, BDKRB2 participates in BK-induced anion secretion in epididymal and vas deferens epithelial cells [7, 8] and in BK-dependent prostaglandin production in the vas deferens [9]. Whereas *Bdkrb2* mRNA expression had been described in the whole epididymis [32], there was no evidence to date on the presence of this receptor in epithelial cells of this organ at the protein level. In the present study, we show that only BDKRB2 (and not BDKRB1) is expressed in epithelial cells of the epididymis.

Activation of BDKRB2 by BK initiates a Ca^{2+} release from intracellular stores via IP_3-gated Ca^{2+} channels, followed by protein kinase C (PKC) activation [5, 48]. In the present study, we show that BK-induced glycerol transport in tubules isolated from the distal initial segment is counteracted by addition of the calcium chelator BAPTA-AM, indicating the participation of calcium in this process. This result is consistent with the

work of Cheuk et al. [7], which shows that the activation of anion secretion by apical Lys-BK in epididymal cultured cells requires intracellular Ca^{2+}.

Our results show that AQP9 and BDKRB2 are expressed in the same cell subtypes in some regions of the male reproductive tract (i.e., nonciliated cells in the efferent ducts and principal cells in the distal initial segment, corpus, and cauda epididymidis), where they colocalize in the apical membrane. While a uniform *Bdkrb2* mRNA expression was detected along the efferent ducts and epididymal tubule, significant variations in the expression of BDKRB2 were detected in specific regions. Discrepancy between mRNA and protein expression levels is a generalized phenomenon that is due to a variety of factors, including posttranslational regulation of the gene and/or rapid turnover of the protein [49]. Additional studies will be required to further characterize regulation of the segmental expression of BDKRB2 in the

FIG. 7.   Triple immunostaining for AQP9 (**B**; green), BDKRB2 (**C**; red), and the ATP6V1E1 (**D**; blue). **A**) Merged panel showing that BDKRB2 colocalizes with AQP9 in the apical membrane of principal cells (yellow) and is absent from clear cells (blue). Nuclei were counterstained with DAPI and are shown in pink by including them in the red and blue channels simultaneously using Photoshop. Bars = 30 μm.
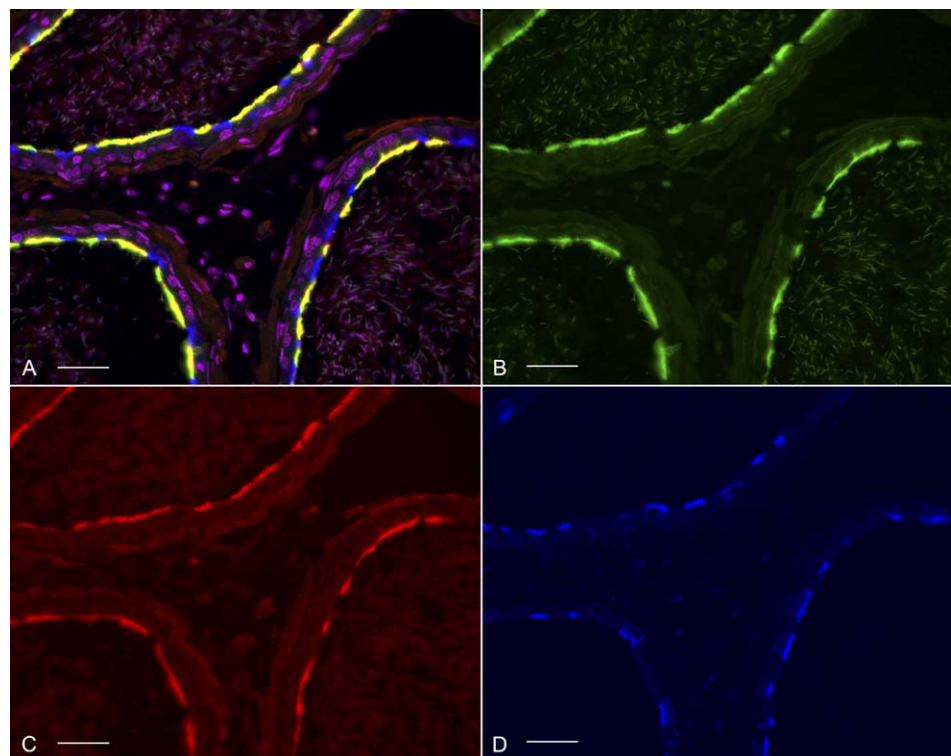
different segments of the epididymis. The highest expression was detected in the efferent ducts and cauda epididymidis, but in some other regions no BDKRB2 labeling was detected. Because AQP9 is highly expressed in all segments of the epididymis (for review see [28]), these results indicate that factors other than BK might also play a role in the regulation of this channel. Our study nevertheless shows that in segments where both BDKRB2 and AQP9 are coexpressed in principal cells (e.g., the distal initial segment), BK does activate AQP9-dependent glycerol permeability.

In the kidney, BK regulates aquaporin 2 recycling via BDKRB2 in a Rho-dependent manner [50]. In the epididymis, AQP9 is not regulated by recycling between the plasma membrane and intracellular vesicles [30], and BK must, therefore, regulate AQP9 via a different mechanism. We have recently shown that SLC9A3R1 (also known as NHERF1, Na/H Exchanger Regulatory Factor) and CFTR (Cystic Fibrosis Transmembrane conductance Regulator)—also expressed in the apical membrane of principal and nonciliated cells [51]—facilitates the activation of AQP9 by cAMP [25]. CFTR is regulated via its interaction with SLC9A3R1, and it was proposed that phosphorylation of SLC9A3R1 by PKC would switch CFTR from being an active chloride channel to a regulatory protein [52]. Therefore, it remains possible that the BK-induced elevation of calcium might contribute to the activation of AQP9 by favoring its regulation by CFTR. Future studies will be required to determine whether BK participates in the interplay between SLC9A3R1, CFTR, and AQP9. Alternatively, a direct activation of AQP9 by PKC remains possible, as several putative serine and tyrosine phosphorylation sites are present in the cytoplasmic COOH- and NH$_2$-terminal tails of AQP9.

Role of BK in the Integrated Function of the Epididymis

Previous studies have shown that the low molecular weight kininogen precursor (LMWK) is expressed in the testis [53] and that tissue kallikrein (tK) is present in germ cells and in the apical surface of epididymal epithelial cells [32]. Our data now show a high level of BK (2 nM) in the lumen of the epididymis compared to the plasma concentration, which is in the picomolar range [54]. Similar high concentrations of BK were also observed in the saliva and cerebrospinal fluid [55, 56], further indicating an important role for luminal BK in the regulation of secretory organs. In the male reproductive tract, BK could be formed in the testis by the action of germ cell tK on LMWK and be subsequently delivered to the efferent ducts and epididymis via the rete testis. Alternatively, BK could be produced directly in the epididymis by the action of local tK on secreted testicular LMWK. In rats, BK but not Lys-BK has been found in urine, blood, and tissue [57, 58], and degradation of rat kininogens by glandular kallikrein can only generate BK [59].

Interestingly, the KKS works in concert with the renin-angiotensin system. While angiotensin-converting enzyme (ACE) converts angiotensin 1 to angiotensin 2, it also contributes to the degradation of BK. The germinal form of ACE (gACE) is abundantly expressed in the membrane of spermatozoa as an anchored protein and is released into the epididymal fluid of several mammals during passage of spermatozoa through the anterior caput epididymidis [60]. ACE knockout male mice are infertile due to the poor quality of their spermatozoa, which are unable to fertilize an egg [61–63]. Germinal ACE has a very high affinity for BK in vitro [64]. The release of gACE from spermatozoa might, therefore, play a role in the regulation of AQP9 by BK by providing a negative feedback mechanism. In this respect, AQP9 activity
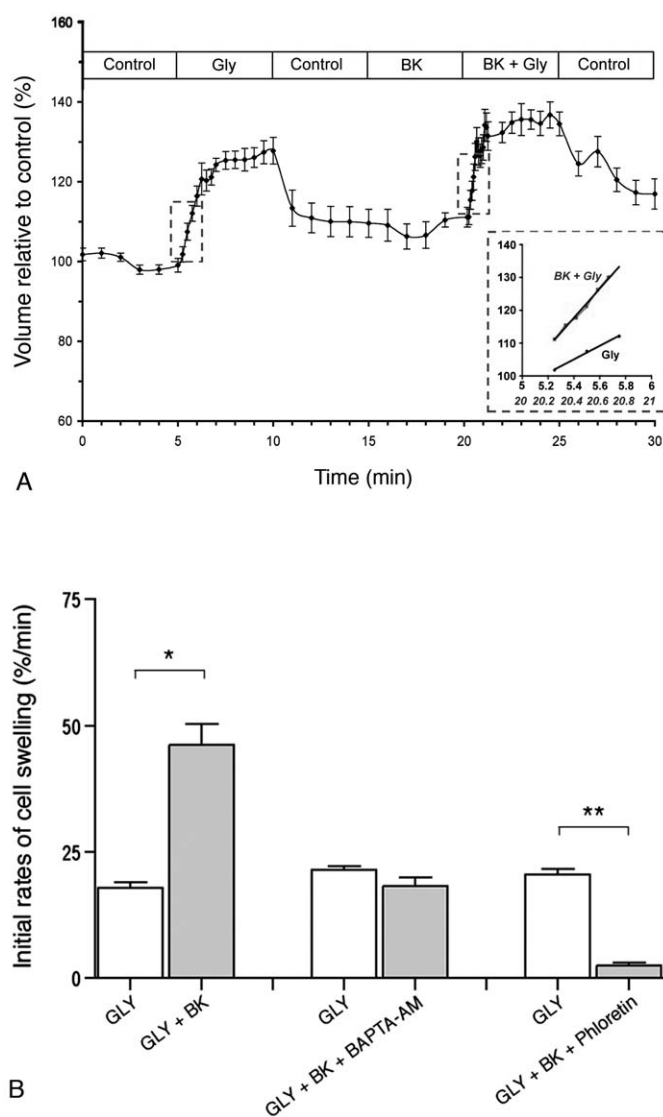

FIG. 8.   Effect of BK on the initial rate of cell swelling induced by luminal isotonic addition of glycerol on tubules isolated from the distal initial segment. **A**) Global profile of cell volume variations induced upon replacement of 60 mM raffinose with glycerol (Gly). After a postcontrol period of 5 min in the absence of glycerol (Control), BK was added into the luminal perfusate (BK) for a period of 5 min, followed by a second pulse of glycerol still in the presence of BK (BK + Gly). Inset: Initial rates of cell swelling measured during the first minute of both glycerol pulses (highlighted by the dashed lines). Data are mean ± SEM (n = 7). **B**) Left bars: Initial rates of glycerol-induced cell swelling measured under control conditions (GLY) and in the presence of 1 μM BK (GLY + BK; n = 7). Middle bars: Initial rates of cell swelling under control condition (GLY) or in the presence of BK and 5 μM BAPTA-AM (GLY + BK + BAPTA-AM; n = 9). Right bars: Control (GLY) or BK plus phloretin (GLY + BK + Phloretin; n = 7). Data are mean ± SEM. *$P < 0.001$; **$P < 0.0005$. Student t-test was used for paired experiments.

might be expected to be higher in the efferent ducts and distal initial segment, where BDKRB2 is expressed, and where gACE is still anchored to the sperm membrane. In these regions the local concentration of BK near the surface of the epithelium may be higher compared to the more distal regions of the epididymis. Interestingly, BDKRB2 expression drops abruptly from the efferent ducts to the proximal initial segment, indicating that BK is not an important luminal regulator in this specific region. AQP9 is not only permeant to solutes, but it is also a water channel. Thus, a higher local concentration of BK

in the efferent ducts would correlate with the very high water transport properties of this organ, which reabsorbs the bulk of water that originates from the testis [14, 16, 17]. In the corpus and cauda epididymidis, where BDKRB2 is also expressed, activation of AQP9 by BK might work in concert with the stimulation of anion secretion by this hormone, which was previously revealed in epididymal epithelial cells in culture [7]. In the distal epididymis, chloride secretion via CFTR drives transepithelial water transport [22]. The concerted regulation of AQP9 and CFTR by BK might, therefore, help control the final fluidity of the epididymal luminal content.

In summary, we have characterized the expression of BDKRB2 in the male reproductive tract and demonstrated the role of BK in glycerol and potentially water transport via AQP9. We also showed that the activation of AQP9 by luminal BK is calcium dependent. These data point to a regulatory role for BK in modulating the luminal environment in the excurrent duct system, which may be important for the development and maintenance of male fertility.

ACKNOWLEDGMENT

REFERENCES

1. Mukai H, Fitzgibbon WR, Bozeman G, Margolius HS, Ploth DW. Bradykinin B2 receptor antagonist increases chloride and water absorption in rat medullary collecting duct. Am J Physiol 1996; 271:R352–R360.
2. Rowland NE, Fregly MJ, Cimmerer AL. Bradykinin-induced water intake and brain fos-like immunoreactivity in rats. Brain Res 1995; 669:73–78.
3. Bhoola KD, Figueroa CD, Worthy K. Bioregulation of kinins: kallikreins, kininogens, and kininases. Pharmacol Rev 1992; 44:1–80.
4. Prado GN, Taylor L, Zhou X, Ricupero D, Mierke DF, Polgar P. Mechanisms regulating the expression, self-maintenance, and signaling-function of the bradykinin B2 and B1 receptors. J Cell Physiol 2002; 193:275–286.
5. Leeb-Lundberg LM, Marceau F, Muller-Esterl W, Pettibone DJ, Zuraw BL. International union of pharmacology. XLV. Classification of the kinin receptor family: from molecular mechanisms to pathophysiological consequences. Pharmacol Rev 2005; 57:27–77.
6. Atanassova N, Kancheva L, Somlev B. Bradykinin stimulates prepubertal rat germ cell proliferation in vitro. Immunopharmacology 1998; 40:173–178.
7. Cheuk BL, Ko WH, Wong PY. COX-dependent and -independent pathways in bradykinin-induced anion secretion in rat epididymis. J Cell Physiol 2002; 191:217–226.
8. Pierucci-Alves F, Schultz BD. Bradykinin-stimulated cyclooxygenase activity stimulates vas deferens epithelial anion secretion in vitro in swine and humans. Biol Reprod 2008; 79:501–509.
9. Peredo HA, Celuch SM. Bradykinin and electrical stimulation increase prostaglandin production in the rat vas deferens. Prostaglandins Leukot Essent Fatty Acids 2001; 65:9–14.
10. Kaneko S, Moriwaki C. Effects of kinins and dipeptidyl carboxypeptidase on the motility of highly washed human sperm. J Pharmacobiodyn 1981; 4:443–450.
11. Schill WB, Miska W. Possible effects of the kallikrein-kinin system on male reproductive functions. Andrologia 1992; 24:69–75.
12. Somlev B, Subev M. Effect of kininase II inhibitors on bradykinin-stimulated bovine sperm motility. Theriogenology 1998; 50:651–657.
13. Cheung KH, Leung GP, Leung MC, Shum WW, Zhou WL, Wong PY. Cell-cell interaction underlies formation of fluid in the male reproductive tract of the rat. J Gen Physiol 2005; 125:443–454.
14. Clulow J, Hansen LA, Jones RC. In vivo microperfusion of the ductuli efferentes testis of the rat: flow dependence of fluid reabsorption. Exp Physiol 1996; 81:633–644.
15. Clulow J, Jones RC, Hansen LA. Micropuncture and cannulation studies of fluid composition and transport in the ductuli efferentes testis of the rat: comparisons with the homologous metanephric proximal tubule. Exp Physiol 1994; 79:915–928.
16. Clulow J, Jones RC, Hansen LA, Man SY. Fluid and electrolyte reabsorption in the ductuli efferentes testis. J Reprod Fertil Suppl 1998; 53:1–14.
17. Hess RA. Oestrogen in fluid transport in efferent ducts of the male reproductive tract. Rev Reprod 2000; 5:84–92.
18. Johnson AL, Howards SS. Hyperosmolality in intraluminal fluids from hamster testis and epididymis: a micropuncture study. Science 1977; 195:492–493.
19. Levine N, Marsh DJ. Micropuncture studies of the electrochemical aspects of fluid and electrolyte transport in individual seminiferous tubules, the epididymis and the vas deferens in rats. J Physiol 1971; 213:557–570.
20. Turner TT, Cesarini DM. The ability of the rat epididymis to concentrate spermatozoa. Responsiveness to aldosterone. J Androl 1983; 4:197–202.
21. Sedlacek RL, Carlin RW, Singh AK, Schultz BD. Neurotransmitter-stimulated ion transport by cultured porcine vas deferens epithelium. Am J Physiol Renal Physiol 2001; 281:F557–F570.
22. Wong PY. CFTR gene and male fertility. Mol Hum Reprod 1998; 4:107–110.
23. Cooper TG, Brooks DE. Entry of glycerol into the rat epididymis and its utilization by epididymal spermatozoa. J Reprod Fertil 1981; 61:163–169.
24. Cheung KH, Leung CT, Leung GP, Wong PY. Synergistic effects of cystic fibrosis transmembrane conductance regulator and aquaporin-9 in the rat epididymis. Biol Reprod 2003; 68:1505–1510.
25. Pietrement C, Da Silva N, Silberstein C, James M, Marsolais M, Van Hoek A, Brown D, Pastor-Soler N, Ameen N, Laprade R, Ramesh V, Breton S. Role of NHERF1, cystic fibrosis transmembrane conductance regulator, and cAMP in the regulation of aquaporin 9. J Biol Chem 2008; 283:2986–2996.
26. Tsukaguchi H, Shayakul C, Berger UV, Mackenzie B, Devidas S, Guggino WB, van Hoek AN, Hediger MA. Molecular characterization of a broad selectivity neutral solute channel. J Biol Chem 1998; 273:24737–24743.
27. Badran HH, Hermo LS. Expression and regulation of aquaporins 1, 8, and 9 in the testis, efferent ducts, and epididymis of adult rats and during postnatal development. J Androl 2002; 23:358–373.
28. Da Silva N, Pietrement C, Brown D, Breton S. Segmental and cellular expression of aquaporins in the male excurrent duct. Biochim Biophys Acta 2006; 1758:1025–1033.
29. Elkjaer M, Vajda Z, Nejsum LN, Kwon T, Jensen UB, Amiry-Moghaddam M, Frokiaer J, Nielsen S. Immunolocalization of AQP9 in liver, epididymis, testis, spleen, and brain. Biochem Biophys Res Commun 2000; 276:1118–1128.
30. Pastor-Soler N, Bagnis C, Sabolic I, Tyszkowski R, McKee M, Van Hoek A, Breton S, Brown D. Aquaporin 9 expression along the male reproductive tract. Biol Reprod 2001; 65:384–393.
31. Monsees TK, Blocher S, Heidorn F, Winkler A, Siems WE, Muller-Esterl W, Hayatpour J, Miska W, Schill WB. Expression and location of the bradykinin B2 receptor in rat testis. Biol Reprod 2002; 67:1832–1839.
32. Monsees TK, Blocher S, Loddo C, Steger K, Schill WB. Tissue kallikrein and bradykinin B2 receptors in the reproductive tract of the male rat. Andrologia 2003; 35:24–31.
33. Beaulieu V, Da Silva N, Pastor-Soler N, Brown CR, Smith PJ, Brown D, Breton S. Modulation of the actin cytoskeleton via gelsolin regulates vacuolar H+-ATPase recycling. J Biol Chem 2005; 280:8452–8463.
34. Pastor-Soler N, Beaulieu V, Litvin TN, Da Silva N, Chen Y, Brown D, Buck J, Levin LR, Breton S. Bicarbonate-regulated adenylyl cyclase (sAC) is a sensor that regulates pH-dependent V-ATPase recycling. J Biol Chem 2003; 278:49523–49529.
35. Pastor-Soler NM, Hallows KR, Smolak C, Gong F, Brown D, Breton S. Alkaline pH- and cAMP-induced V-ATPase membrane accumulation is mediated by protein kinase A in epididymal clear cells. Am J Physiol Cell Physiol 2008; 294:C488–C494.
36. Da Silva N, Shum WW, El-Annan J, Paunescu TG, McKee M, Smith PJ, Brown D, Breton S. Relocalization of the V-ATPase B2 subunit to the apical membrane of epididymal clear cells of mice deficient in the B1 subunit. Am J Physiol Cell Physiol 2007; 293:C199–C210.
37. Herak-Kramberger CM, Breton S, Brown D, Kraus O, Sabolic I. Distribution of the vacuolar H+ ATPase along the rat and human male reproductive tract. Biol Reprod 2001; 64:1699–1707.
38. Pietrement C, Sun-Wada GH, Silva ND, McKee M, Marshansky V, Brown D, Futai M, Breton S. Distinct expression patterns of different subunit isoforms of the V-ATPase in the rat epididymis. Biol Reprod 2006; 74:185–194.
39. Pastor-Soler N, Isnard-Bagnis C, Herak-Kramberger C, Sabolic I, Van Hoek A, Brown D, Breton S. Expression of aquaporin 9 in the adult rat epididymal epithelium is modulated by androgens. Biol Reprod 2002; 66:1716–1722.
40. Bagnis C, Marsolais M, Biemesderfer D, Laprade R, Breton S. Na+/H+-exchange activity and immunolocalization of NHE3 in rat epididymis. Am J Physiol Renal Physiol 2001; 280:426–436.

41. Jensen LJ, Stuart-Tilley AK, Peters LL, Lux SE, Alper SL, Breton S. Immunolocalization of AE2 anion exchanger in rat and mouse epididymis. Biol Reprod 1999; 61:973–980.

42. Brown D, Lydon J, McLaughlin M, Stuart-Tilley A, Tyszkowski R, Alper S. Antigen retrieval in cryostat tissue sections and cultured cells by treatment with sodium dodecyl sulfate (SDS). Histochem Cell Biol 1996; 105:261–267.

43. Breton S, Wiederhold T, Marshansky V, Nsumu NN, Ramesh V, Brown D. The B1 subunit of the H+ATPase is a PDZ domain-binding protein. Colocalization with NHE-RF in renal B-intercalated cells. J Biol Chem 2000; 275:18219–18224.

44. Da Silva N, Silberstein C, Beaulieu V, Pietrement C, Van Hoek AN, Brown D, Breton S. Postnatal expression of aquaporins in epithelial cells of the rat epididymis. Biol Reprod 2006; 74:427–438.

45. Blaukat A. Structure and signalling pathways of kinin receptors. Andrologia 2003; 35:17–23.

46. Blaukat A, Alla SA, Lohse MJ, Muller-Esterl W. Ligand-induced phosphorylation/dephosphorylation of the endogenous bradykinin B2 receptor from human fibroblasts. J Biol Chem 1996; 271:32366–32374.

47. Regoli D. Neurohumoral regulation of precapillary vessels: the kallikrein-kinin system. J Cardiovasc Pharmacol 1984; 6(suppl 2):S401–S412.

48. Dixon BS, Sharma RV, Dickerson T, Fortune J. Bradykinin and angiotensin II: activation of protein kinase C in arterial smooth muscle. Am J Physiol 1994; 266:C1406–C1420.

49. Kozak M. Some thoughts about translational regulation: forward and backward glances. J Cell Biochem 2007; 102:280–290.

50. Tamma G, Carmosino M, Svelto M, Valenti G. Bradykinin signaling counteracts cAMP-elicited aquaporin 2 translocation in renal cells. J Am Soc Nephrol 2005; 16:2881–2889.

51. Leung GP, Gong XD, Cheung KH, Cheng-Chew SB, Wong PY. Expression of cystic fibrosis transmembrane conductance regulator in rat efferent duct epithelium. Biol Reprod 2001; 64:1509–1515.

52. Yoo D, Flagg TP, Olsen O, Raghuram V, Foskett JK, Welling PA. Assembly and trafficking of a multiprotein ROMK (Kir 1.1) channel complex by PDZ interactions. J Biol Chem 2004; 279:6863–6873.

53. Takano M, Kondo J, Yayama K, Otani M, Sano K, Okamoto H. Molecular cloning of cDNAs for mouse low-molecular-weight and high-molecular-weight prekininogens. Biochim Biophys Acta 1997; 1352:222–230.

54. Scott AC, Wensel R, Davos CH, Georgiadou P, Ceri Davies L, Coats AJ, Francis DP, Piepoli MF. Putative contribution of prostaglandin and bradykinin to muscle reflex hyperactivity in patients on Ace-inhibitor therapy for chronic heart failure. Eur Heart J 2004; 25:1806–1813.

55. Chen Y, Xu L, Lin J, Chen G. Assay of bradykinin-related peptides in human body fluids using capillary electrophoresis with laser-induced fluorescence detection. Electrophoresis 2008; 29:1302–1307.

56. Vickers ER, Goebel C, Mather LE, Mackay L, Wells RJ. High-performance liquid chromatographic determination of bradykinin in saliva: a critical review and a new method. J Chromatogr B Biomed Sci Appl 2001; 755:101–110.

57. Campbell DJ, Kladis A, Duncan AM. Bradykinin peptides in kidney, blood, and other tissues of the rat. Hypertension 1993; 21:155–165.

58. Hagiwara Y, Kojima M, Kuraishi T, Hayashi I, Miyata T, Oh-ishi S. Identification of rat urinary kinin as bradykinin. Life Sci 1995; 57:997–1002.

59. Kato H, Enjyoji K, Miyata T, Hayashi I, Oh-ishi S, Iwanaga S. Demonstration of arginyl-bradykinin moiety in rat HMW kininogen: direct evidence for liberation of bradykinin by rat glandular kallikreins. Biochem Biophys Res Commun 1985; 127:289–295.

60. Gatti JL, Druart X, Guerin Y, Dacheux F, Dacheux JL. A 105- to 94-kilodalton protein in the epididymal fluids of domestic mammals is angiotensin I-converting enzyme (ACE); evidence that sperm are the source of this ACE. Biol Reprod 1999; 60:937–945.

61. Esther CR Jr, Howard TE, Marino EM, Goddard JM, Capecchi MR, Bernstein KE. Mice lacking angiotensin-converting enzyme have low blood pressure, renal pathology, and reduced male fertility. Lab Invest 1996; 74:953–965.

62. Hagaman JR, Moyer JS, Bachman ES, Sibony M, Magyar PL, Welch JE, Smithies O, Krege JH, O'Brien DA. Angiotensin-converting enzyme and male fertility. Proc Natl Acad Sci U S A 1998; 95:2552–2557.

63. Krege JH, John SW, Langenbach LL, Hodgin JB, Hagaman JR, Bachman ES, Jennette JC, O'Brien DA, Smithies O. Male-female differences in fertility and blood pressure in ACE-deficient mice. Nature 1995; 375:146–148.

64. Metayer S, Dacheux F, Guerin Y, Dacheux JL, Gatti JL. Physiological and enzymatic properties of the ram epididymal soluble form of germinal angiotensin I-converting enzyme. Biol Reprod 2001; 65:1332–1339.